


Erratum: Atomistic analysis of Auger recombination in *c*-plane (In,Ga)N/GaN quantum wells: Temperature-dependent competition between radiative and nonradiative recombination
[Phys. Rev. B **105**, 195307 (2022)]Joshua M. McMahon , Emmanouil Kioupakis, and Stefan Schulz

(Received 21 June 2023; published 7 July 2023)

DOI: [10.1103/PhysRevB.108.039901](https://doi.org/10.1103/PhysRevB.108.039901)

Upon reexamining our published results, we discovered that the data plotted and discussed were in the absence of the screening parameter α of the Coulomb interaction given in Eq. (2) and after Eq. (4) of the original paper. Overall, the correction from the screening mainly resulted in quantitative shifts of the results, but essentially none of the conclusions of the original paper are impacted. With the temperature-dependent screening parameter α included, the

(1) hole-hole-electron Auger rate still dominates the total Auger rate for all three In contents studied. The main influence of Coulomb screening is that the smaller electron-electron-hole Auger coefficient is reduced even further. In the 10% and 15% In quantum well systems, this effect is of secondary importance as the electron-electron-hole Auger coefficients already only contributed $< 1\%$ to the total coefficient in the original paper. Only the quantum well system with 25% In was affected, reducing the electron-electron-hole contribution to now also just 1% across the entire temperature range studied. In Fig. 1 below, we show the corrected data. We note that these changes do not affect the conclusion of the paper that alloy-enhanced Auger recombination may not present an intrinsic roadblock to achieving efficient recombination in the green to yellow range.

(2) Total (averaged) Auger coefficients range from $\approx 4 \times 10^{-30}$ (10% In) to $\approx 2 \times 10^{-31}$ -cm⁶/s (25%) at a temperature of 300 K and a carrier density of $n_{3D} = 3.8 \times 10^{18}$ cm⁻³ where n_{3D} represents the volume carrier density, which is slightly reduced compared to the data given in the original paper (which ranged from $\approx 6 \times 10^{-30}$ to $\approx 3 \times 10^{-31}$ cm⁶/s at a temperature of 300 K and a carrier density of $n_{3D} = 3.8 \times 10^{18}$ cm⁻³); see also Fig. 2 in this Erratum. The hole-hole-electron Auger coefficients are only weakly affected by the Coulomb screening given that they are dominated by localized hole states (see Fig. 3 in this Erratum for an example of the corrected hole-hole-electron Auger coefficients C_{hhe} , in the 15% In quantum well). Overall, the corrected total coefficients are still large enough to significantly impact the efficiency of (In,Ga)N based quantum well systems as discussed in the original paper. The comparison with available literature data is shown Fig. 4 of this Erratum. Thus, none of the conclusions in the original paper are affected.

(3) Auger coefficients still exhibit a weak temperature dependence as shown in Fig. 5 of this Erratum, in line with the conclusion of the original paper.

(4) Ratio of radiative to nonradiative (Auger) recombination in the temperature range relevant to the thermal droop still increases as Fig. 5 of this Erratum shows. Thus, the conclusion of the original paper that the competition between radiative and Auger recombination is not driving the thermal droop effect in *c* plane (In,Ga)N/GaN quantum wells is unaffected.

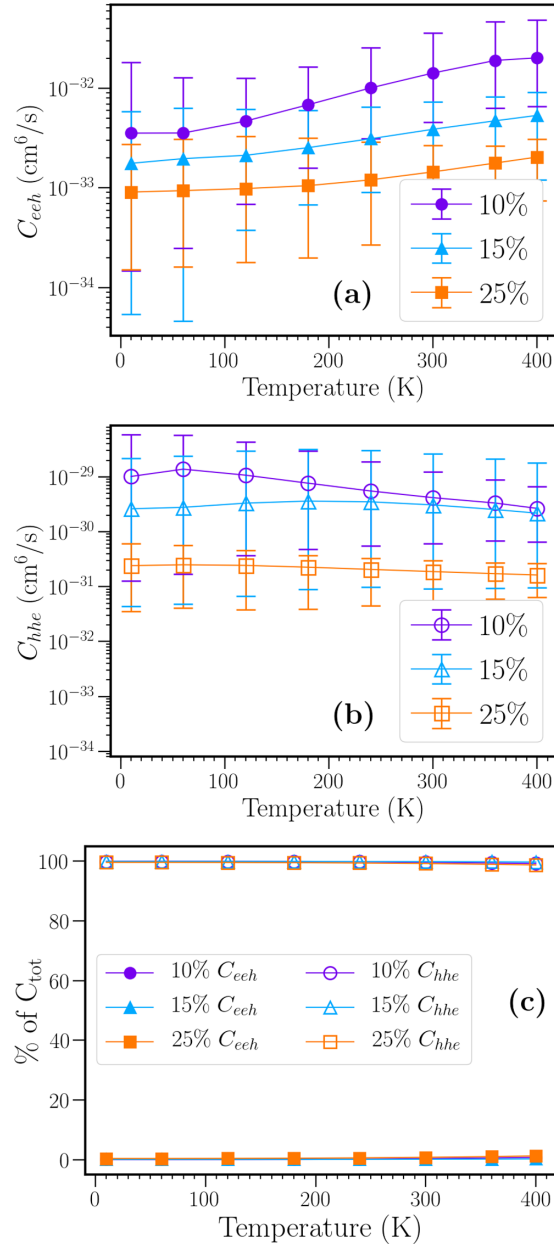


FIG. 1. (a) Electron-electron-hole C_{eeh} , and (b) hole-hole-electron C_{hhe} , Auger coefficients as a function of temperature T for c -plane (In,Ga)N/GaN quantum wells with different In contents (10%, 15%, and 25%). The data, averaged over ten microscopic alloy configurations, are given by the filled (C_{eeh}) and open (C_{hhe}) symbols; error bars indicate maximum and minimum values of C_λ ($\lambda = \{eeh, hhe\}$) at a given temperature. The calculations have been carried out at a fixed carrier density of $n_{3D} = 3.8 \times 10^{18} \text{ cm}^{-3}$. (c) Percentage breakdown of the contribution from C_{eeh} and C_{hhe} to the total Auger coefficient C_{tot} . Replaces Fig. 1 in the original paper.

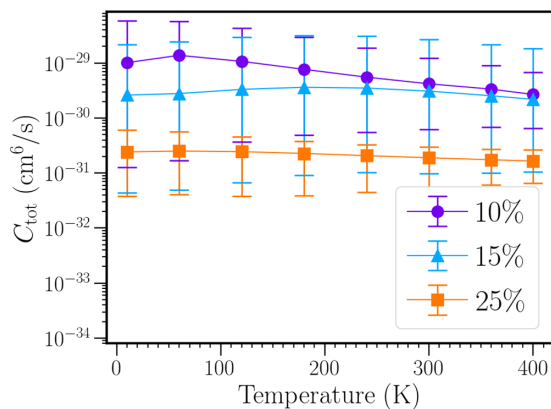


FIG. 2. Total Auger coefficient C_{tot} as a function of temperature T for c -plane (In,Ga)N/GaN quantum wells with different In contents (10%, 15%, and 25%). The data, averaged over ten microscopic configurations are given by the filled symbols; error bars indicate maximum and minimum values of C_{tot} at a given temperature, across the ten configurations. The calculations have been carried out at a fixed carrier density of $n_{3D} = 3.8 \times 10^{18} \text{ cm}^{-3}$. Replaces Fig. 2 in the original paper.

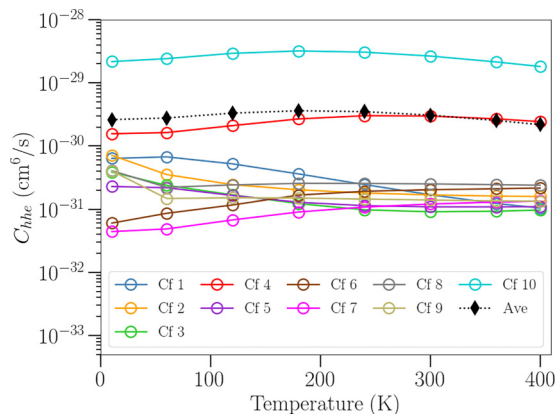


FIG. 3. Auger coefficient C_{hhe} as a function of temperature T for each of the ten different alloy configurations (Cfs) for the 15% In quantum well system. The black diamonds denote the coefficient when averaging over the ten different alloy configurations. The calculations have been carried out at a fixed carrier density of $n_{3D} = 3.8 \times 10^{18} \text{ cm}^{-3}$. Replaces Fig. 6 in the original paper.

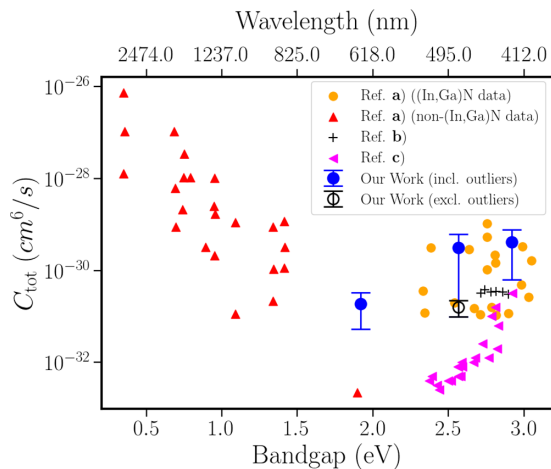


FIG. 4. Comparison of calculated and measured Auger coefficients (C_{tot}) as a function of (effective) band gap and emission wavelength. Data from several literature sources are included (see original paper). Replaces Fig. 3 in the original paper.

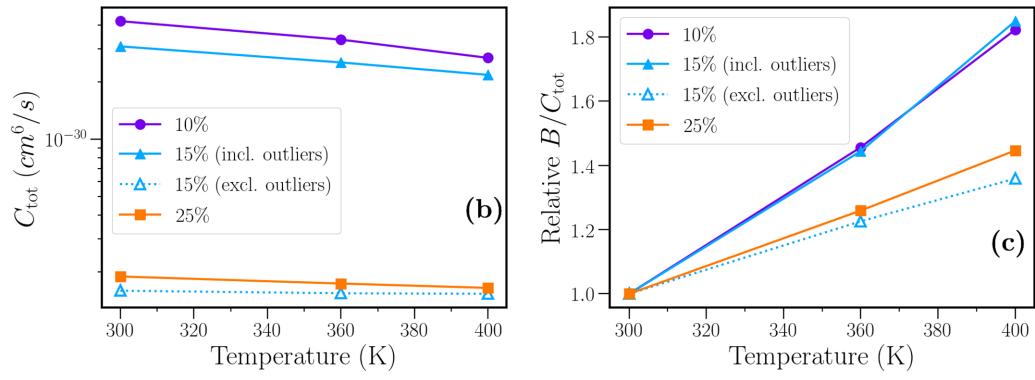


FIG. 5. (b) Total nonradiative Auger coefficient C_{tot} , and (c) ratio of radiative B and Auger C_{tot} coefficients B/C_{tot} relative to B/C_{tot} at 300 K as a function of temperature (above 300 K) for 10%, 15%, and 25% In in the well. The carrier density is fixed at $n_{3D} = 3.8 \times 10^{18} \text{ cm}^{-3}$. Replaces Figs. 4(b) and 4(c) in the original paper; Fig. 4(a) in the original paper is unaffected.